XL CILAMCE
IBERO-LATIN AMERICAN CONGRESS ON COMPUTATIONAL METHODS IN ENGINEERING
NOVEMBER 11-14, 2019
Praiamar Natal Hotel & Convention
Natal, RN-BRAZIL

DYNAMIC ANALYSIS OF A BUILDING UNDER SEISMIC EXCITATION

Raiza Michele Guimarães
Tiago Wagner Dada
Eduardo Pagnussat Titello
Natalia Pinheiro da Silva
Livio Pires de Caravalho Melo
raizaguimaraesmt@gmail.com
tiagowdada@gmail.com
eduardotitello@gmail.com
pinheiros.natalia@gmail.com
liviopires@gmail.com
Master's degree students in Structural Engineering, Department of Civil Engineering, Federal University of Rio Grande do Sul
99 Osvaldo Aranha Ave, 90035-190, Porto Alegre/RS, Brazil
Leticia Fleck Fadel Miguel
letffm@ufrgs.br
Department of Mechanical Engineering, Federal University of Rio Grande do Sul
425 Sarmento Leite St, 90050-170, Porto Alegre/RS, Brazil

Abstract. This paper implemented a numerical routine in MATLAB software to analyze the dynamic response of a building with several degrees of freedom excited by seismic motion. The loading was modeled as a one-dimensional stochastic process, which was simulated by passing a Gaussian white noise process through a Kanai-Tajimi filter. Parameters of ground motion such as frequency, damping and peak acceleration were considered taking into account a region located in Chile where the seismic problem is of great importance, and another one taken from a region of Brazil that has the largest seismic activity for this country. The ground acceleration, in the frequency domain, was generated by Kanai-Tajimi spectrum and it was transformed into the time domain by the Shinozuka & Jan Method. The structure analyzed is a 12-story building modeled as a two-dimensional finite element discretized into frame elements. The structural damping model considered was the Rayleigh model and the mass consistent matrix was adopted. The structural dynamic motion equation was solved by the Newmark Method and the maximum values, in absolute values, of the displacements, accelerations and the inter-story drift of the building were calculated. A maximum value established by national codes for the inter-story drift was considered as a limiting parameter for structural damage. The results indicate that major damages are obtained when the frequencies of the site condition were closed to the natural frequencies of the first three vibration modes of the structure.

Keywords: Dynamic Analysis, Seismic excitation, Kanai-Tajimi, Newmark Method

1 Introduction

Dynamic effects over buildings can be a decisive factor in the structural design process. In regions under high seismic action, considering these effects on the structural project is even more relevant. Even though Brazil is mostly not an active seismic zone, significant earthquakes occur in some parts of the country, making it substantial to study these effects on structures.

The main objectives of this study are to model a simplified real structure, generating a seismic excitation signal and analyzing the structure's response to the seismic motion.

2 Linear Dynamic Analysis

2.1 Equation of motion

The movement equation of a system, with multiple degrees of freedom, under a seismic excitation on its base is given by Clough and Penzien [1]:

$$[M]\{\ddot{x}_t\} + [C]\{\dot{x}_t\} + [K]\{x_t\} = \{F_t\} \tag{1}$$

Where [M], [C] and [K] are the *nxn* size structural mass, damping and stiffness matrices, respectively, of the *n* degrees of freedom number. The parameters $\ddot{x}_t$, $\dot{x}_t$, x_t correspond, successively, to the acceleration, velocity and displacement vectors of the degrees of freedom in relation to the base. The independent factor in the movement $\{F_t\}$ is the n-dimensional external forces vector and can be determined by the following expression Miguel et al. [2]:

$$\{F_t\} = -MBa_{g,x}(t) \tag{2}$$

Where B is a *nxd* matrix that contains the cosine directors of the angles formed between the base motion and the direction of the displacement (degree of freedom) considered , *d* is the number of directions of the ground motion and $a_{g,x}(t)$ is the *d*-dimensional ground acceleration vector of the seismic excitation.

The negative sign does not affect the dynamic behavior, and is commonly omitted in the formulation.

2.2 Finite element model

Building model

The structure analyzed is a 12-story building as shown in Fig.1 and Fig. 2.

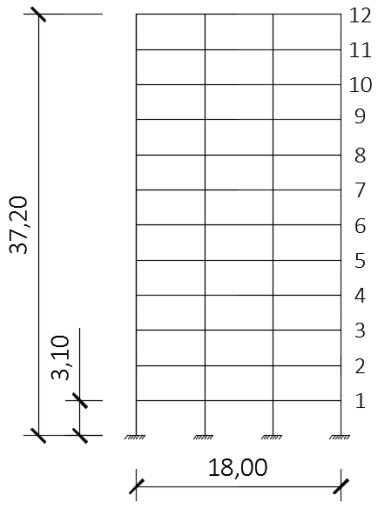

Figure 1. Building frame for analysis

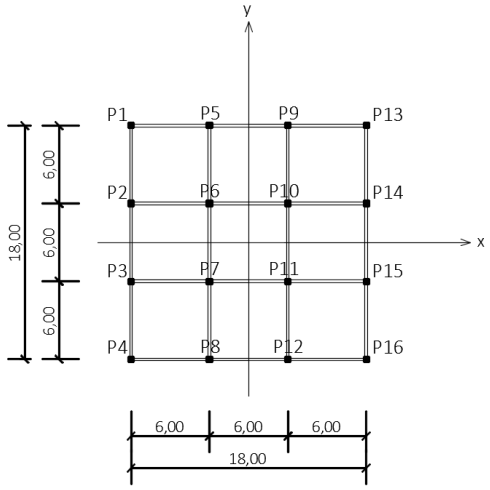

Figure 2. Floor plan view scheme

The geometric properties considered for the structural elements are presented in Table 1.

Table 1. Coefficients in constitutive relations

Structural Elements	Cross section (cm)
Beam	20 x 50
Slab	12 x L
Columns	80 x 80

Where L represents the span of the slab.

A simplified model for the structure is proposed as a two-dimensional finite element discretized into frame elements, where the height and the length of the building are represent by axis z and axis x, respectively.

The simplified model for the floor scheme view is shown in Fig. 3

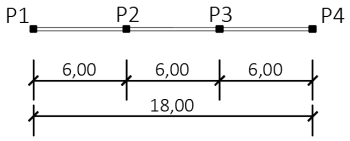

Figure 3. Simplified floor view scheme

This model was built in such manner that the cross-sectional area and mass properties of the original structure would remain.

In order to add the axial stiffness and equivalent mass of the slabs, the cross sectional area of the beams considered the contribution from slabs. However, the bending stiffness of the beams will not receive the contribution from slabs. Since in each direction of the cartesian plane there are four equal frames, the cross-sectional area and the flexural stiffness of the structural elements were calculated by multiplying those properties from the original model by four. Thus, the mass of the columns from the original model is equivalent to the mass of the simplified model. This property is used in the mass matrix elements. The mass of the transverse beams was included by adding this property into the density beam of the reduced model.

The secant modulus of elasticity (Ecs) of the reinforced concrete for the building, class C35 (Fck = 35 MPa), is Ecs = 29 GPa [3]. The following properties in Table 2 were adopted for the equivalent frame. It is noteworthy that the slabs bending stiffness was not considered and only their axial stiffness were taken into account.

Table 2. Summary of the equivalent frame elements properties

Property/Element	Beams	Columns
Area (m^2)	2.46	2.56
Moment of inertia (m^4)	0.008	0.137
Length (m)	6.0	3.1
Mass density (kg/m^3)	2906	2500
Young's modulus (GPa)	29.0	29.0

Frame finite element

Frame elements carry shear forces, bending moments, and axial forces. Each element has two nodes with three degrees of freedom. Adopting the Euler-Bernoulli beam theory, and interpolation functions of the element explained by [4] and [1], the frame element stiffness matrix and mass matrix in local coordinates are given by Eq. 3 and Eq. 4.

$$K^L = \begin{bmatrix} \frac{EA}{L} & 0 & 0 & -\frac{EA}{L} & 0 & 0 \\ 0 & \frac{12EI}{L^3} & \frac{6EI}{L^2} & 0 & -\frac{12EI}{L^3} & \frac{6EI}{L^2} \\ 0 & \frac{6EI}{L^2} & \frac{4EI}{L} & 0 & -\frac{6EI}{L^2} & \frac{2EI}{L} \\ -\frac{EA}{L} & 0 & 0 & \frac{EA}{L} & 0 & 0 \\ 0 & -\frac{12EI}{L^3} & -\frac{6EI}{L^2} & 0 & \frac{12EI}{L^3} & -\frac{6EI}{L^2} \\ 0 & \frac{6EI}{L^2} & \frac{2EI}{L} & 0 & -\frac{6EI}{L^2} & \frac{4EI}{L} \end{bmatrix} \tag{3}$$

$$M^L = \mu A \begin{bmatrix} \frac{L}{3} & 0 & 0 & \frac{L}{6} & 0 & 0 \\ 0 & \frac{13L}{35} & \frac{11L^2}{210} & 0 & \frac{9L}{70} & -\frac{13L^2}{420} \\ 0 & \frac{11L^2}{210} & \frac{L^3}{105} & 0 & \frac{13L^2}{420} & -\frac{L^3}{140} \\ \frac{L}{6} & 0 & 0 & \frac{L}{3} & 0 & 0 \\ 0 & \frac{9L}{70} & \frac{13L^2}{420} & 0 & \frac{13L}{35} & -\frac{11L^2}{210} \\ 0 & -\frac{13L^2}{420} & -\frac{L^3}{140} & 0 & -\frac{11L^2}{210} & \frac{L^3}{105} \end{bmatrix} \tag{4}$$

To transform the element matrices from the local coordinate system to the global coordinate system, the following relation is used:

$$[K^G] = [T^T][K^L][T] \tag{5}$$

$$[M^G] = [T^T][M^L][T] \tag{6}$$

Where [T] is the coordinate transformation matrix expressed by:

$$[T] = \begin{bmatrix} \cos\Theta & \sin\Theta & 0 & 0 & 0 & 0 \\ -\sin\Theta & \cos\Theta & 0 & 0 & 0 & 0 \\ 0 & 0 & 1 & 0 & 0 & 0 \\ 0 & 0 & 0 & \cos\Theta & \sin\Theta & 0 \\ 0 & 0 & 0 & -\sin\Theta & \cos\Theta & 0 \\ 0 & 0 & 0 & 0 & 0 & 1 \end{bmatrix} \tag{7}$$

The degrees of freedom in local coordinates for each node are transformed to global coordinates according to the following equations:

$$gl_{1L}^G = 3N_{No}^G - 2 \tag{8}$$

$$gl_{2L}^G = 3N_{No}^G - 1 \tag{9}$$

$$gl_{3L}^G = 3N_{No}^G \tag{10}$$

Where $3N_{No}^{G}$ represents the node number in the global coordinate system.

Finally, the boundary conditions are applied after eliminating the rigid body movements in the system.

For this dynamic analysis, the Rayleigh damping was assumed, which is proportional to the linear combination of the mass and stiffness matrices, as follows:

$$C = a_0 M + a_1 K \tag{11}$$

Where a_0 and a_1 are constants to be determined from two given damping ratios that correspond to two known frequencies of vibration. The procedure of calculating these coefficients is shown in the following system.

$$\frac{1}{2}\begin{bmatrix} \frac{1}{\omega_i} & \omega_i \\ \frac{1}{\omega_j} & \omega_j \end{bmatrix}\begin{bmatrix} a_0 \\ a_1 \end{bmatrix} = \begin{bmatrix} \xi_i \\ \xi_j \end{bmatrix} \tag{12}$$

Taking into account that the first nature modes of vibration are the major part of the dynamic response [1], the damping for the first and the second mode were established. For both modes, the damping value (critical ratio) of 5% (ξ = 0.05) was adopted, considering as reference the values indicated in literature for buildings submitted to seismic action without vibration isolation systems as in Soriano [5].

2.3 Natural frequencies and mode shapes analysis

The modal parameters refer to the natural modes of vibration and frequencies, which can be determined by considering the free vibration movement equation for multi-degree of freedom undamped systems. This can be properly achieved since the structural damping is usually worthless, not having significant influence over the results Troian [6]. So, the equation of motion in matrix form reduces to:

$$[M]\{\ddot{x}_t\} + [K]\{x_t\} = 0 \tag{13}$$

Assuming that the movement is a harmonic function, multiplied by a vector which defines the modal shape φ, this may be written as $x(t) = \varphi sen(\omega t + \theta)$. When the second time derivative from this relation is applied into the movement equation, the following relation may be expressed:

$$[K - M\omega^2]\varphi = 0 \tag{14}$$

This equation is an eigenvalue problem. The ω^2 terms are the eigenvalue and stand for the problem free-vibration frequencies, whereas φ are the eigenvectors and correspond to the modes of vibration for each frequency. The nontrivial solution of Eq. 14 is:

$$|K - M\omega^2| = 0 \tag{15}$$

Expanding the terms of the determinant from the previous equation generates a new equation, which the *N* roots represent the *N* vibration frequencies of the *N* modes of vibration involved in the problem.

2.4 Seismic Excitation

A seismic excitation simulation can be performed by using real seismic activity measured with accelerograms or by generating artificial earthquakes through the spectral density functions. In a real situation, the local soil properties influence on the excitation dynamic properties conforming to Gomez [7]. The Kanai-Tajimi spectrum includes the characteristics of the overlaying soil deposits in the simulation as stated in [8] and [9].

The ground acceleration on the frequency domain is determined by a one-dimensional stationary stochastic process, passing a Gaussian White noise filter through the Kanai-Tajimi filter, with a power spectral density function described as:

$$S(\omega) = S_0 \left[\frac{\omega_g^4 + 4\omega_g^2 \xi_g^2 \omega^2}{(\omega^2 - \omega_g^2)^2 + 4\omega_g^2 \xi_g^2 \omega^2} \right] \tag{16}$$

Where:

$$S_0 = \frac{0.03\xi_g}{\pi\omega_g(4\xi_g^2 + 1)} \tag{17}$$

In which S_0 is the spectral density constant, ξ_g and ω_g are, respectively, the damping and frequency of the local soil.

The solution of the Eq.16 generates a ground acceleration signal in the frequency domain. To obtain the response in the time domain it is used the method proposed by [10]:

$$a_{g,x}(t) = \sum_{j=1}^{N_\omega} \sqrt{2S(\omega_j)\Delta\omega_j} cos(\omega_j t + \phi_j) \tag{18}$$

Where N_ω is the number of frequency band range; $\Delta\omega_j$ is the frequency increment expressed by $\Delta\omega_j = \omega_{j+1} - \omega_j \phi_j$; ϕ_j indicates the random phase angle with uniform probability distribution function between 0 and 2π; ω_j is the natural frequency in the j^{th} iteration and *t* is the time in seconds.

After obtaining the signal in the time domain, it is necessary to normalize the ground motions to PGA (peak ground acceleration). So, the analysis will be according to the local soil properties in the study.

Based on highly regarded analysis of over 367 earthquakes database, [11] presented the parameters of the Kanai-Tajimi spectrum values for several soil types.

Two different locations were used for generating the seismic signal. In one of them, the building is situated in Santiago, in Chile. Another one is in the northern region of Brazil, in Acre.

Furthermore, the following data was used for both ground acceleration signal to solve the Eq. 18: minimum frequency $f_{min} = 0Hz$, maximum frequency $f_{max} = 25Hz$, frequency increment $\Delta f = 0.01Hz$, initial time $t_0 = 0s$, final time T = 50s, time increment $\Delta = 0.01s$.

2.5 Newmark Method

Bathe [12] presents in his book with details the solution methods for differential equations of displacement for dynamical analysis of linear and non-linear systems. The direct integration and modal superposition are two well-known methods to solve discrete linear systems.

Between the different numerical integration methods one can outline the Implicit Method of Newmark. Characteristically, the equilibrium is considered at time $t + \Delta t$ and not at time *t* for implicit methods.

The method use as supposition that the values of displacement and velocity, when t=0, are given as initial conditions and then the initial acceleration is calculated using the Eq. 19:

$$\ddot{x}(t_0) = M^{-1}[F(t_0) - C\dot{x}(t_0) - Kx(t_0)] \tag{19}$$

For the Newmark method the velocity is calcuted by Eq. 20:

$$\dot{x}(t_{i+1}) = \dot{x}(t_i) + (1-\delta)\Delta t\ddot{x}(t_i) + \delta\Delta t\ddot{x}(t_{i+1}) \tag{20}$$

When the integration process is concluded is possible to evaluate the displacement. This is accomplished by the numerical integration of the previous velocity equation that results the displacement equation given by Eq. 21:

$$x(t_{i+1}) = x(t_i) + \Delta t\dot{x}(t_i) + \left(\frac{1}{2} - \beta\right)\Delta t^2\ddot{x}(t_i) + \beta\Delta t^2\ddot{x}(t_{i+1}) \tag{21}$$

Where δ e $beta$ are parameters that can be determined to obtain integration accuracy stability. Newmark proposed as an unconditionally stable scheme the constant-average-acceleration method, also called trapezoidal rule, in which case $\delta = 1/2$ e $\beta = 1/4$ according to Bathe [12].

A explicit formula to calculate the acceleration is found when $\ddot{x}(t_{i+1})$ from Eq. 21 is in evidence:

$$\ddot{x}(t_{i+1}) = a_0[x(t_{i+1}) - x(t_i)] - a_1x(t_i) - a_2\ddot{x}(t_i) \tag{22}$$

Where:

$$a_0 = \frac{1}{\beta\Delta t^2}, a_1 = \frac{1}{\beta\Delta t}, a_2 = \frac{1}{2\beta} - 1 \tag{23}$$

And the velocity vector is expressed by:

$$\dot{x}(t_{i+1}) = a_3[x(t_{i+1}) - x(t_i)] - a_4x(t_i) - a_5\ddot{x}(t_1) \tag{24}$$

Where:

$$a_3 = \frac{\delta}{\beta\Delta t}, a_4 = \frac{\delta}{\beta} - 1, a_5 = \frac{\Delta t}{2}\left(\frac{\delta}{\beta} - 2\right) \tag{25}$$

Having these values is possible to solve the differential equation of motion from the interval of t=0 to t=T, where T is the time of seismic excitation. The final expressions to calculate the displacements, velocities and accelerations in this method are given, respectively by:

$$x(t_{i+1}) = D\left\{F(t_{i+1}) + M[a_0x(t_i) + a_1\dot{x}(t_i) + a_2\ddot{x}(t_i)] + C[a_3x(t_i) + a_4\dot{x}(t_i) + a_5\ddot{x}(t_i)]\right\} \tag{26}$$

$$D = (a_0 M + a_3 C + K)^{-1} \tag{27}$$

$$\dot{x}(t_{i+1}) = a_3[x(t_{i+1}) - x(t_i)] - a_4\dot{x}(t_i) - a_5\ddot{x}(t_i) \tag{28}$$

$$\ddot{x}(t_{i+1}) = a_0[x(t_{i+1}) - x(t_i)] - a_1\dot{x}(t_i) - a_2\ddot{x}(t_i) \tag{29}$$

3 Algorithm Validation

To validate the algorithm, a building with three floors and two spans, as shown in Fig. 4, was modeled. Columns cross section area is $0.16m^2$ and their moment of inertia is $2.13E10^{-3}m^4$. Beams cross section area is $0.12m^2$ and their moment of inertia is $9.0E10^{-4}m^4$. The material of all the elements is reinforced concrete with Young's modulus of 29 GPa and mass density of 2500 kg/m^3.

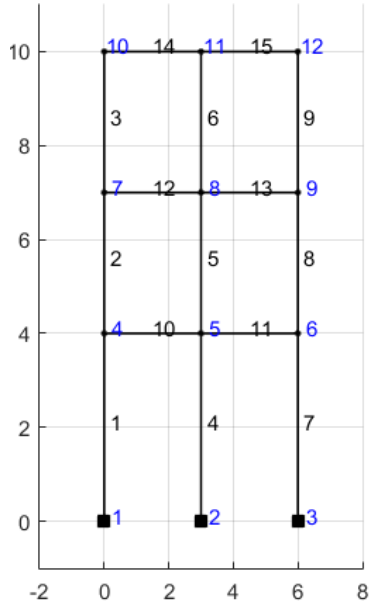

Figure 4. Frame building model for validation

The first five natural frequencies of vibration determined from Ansys software and from the algorithm are presented in Table 3.

Figures 5 and 6 show, respectively, the first mode of vibration obtained from the algorithm produced and from Ansys software.

4 Results and discussions

Once the algorithm was validated, the parameters of the model were entered. Figure 7 shows the 2D model elements and their respective numbering.

With the discretized structure, the frequencies associated with each natural vibration mode of the structure were obtained. By analyzing the power spectrum illustrated in Fig. 8, it is clear that the

Table 3. Comparison of natural frequencies for validation

Modes	Ansys	Algorithm
1° Mode	4.282	4.281
2° Mode	15.254	15.263
3° Mode	31.676	31.740
4° Mode	58.698	58.710
5° Mode	63.673	63.921

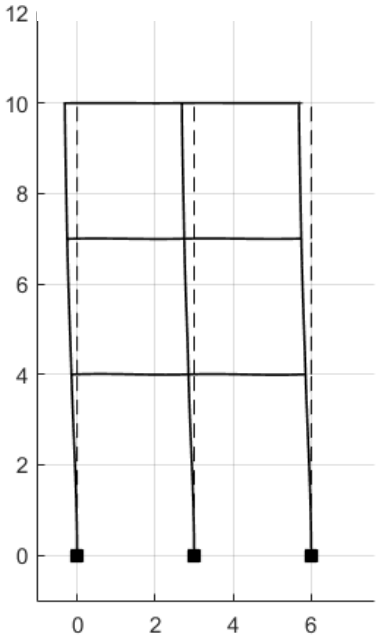

Figure 5. First mode of vibration – 4.28 Hz

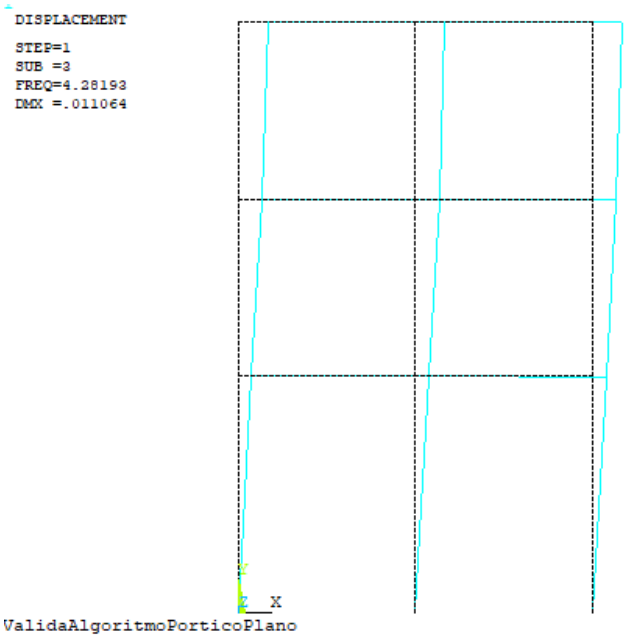

Figure 6. First mode of vibration by Ansys software

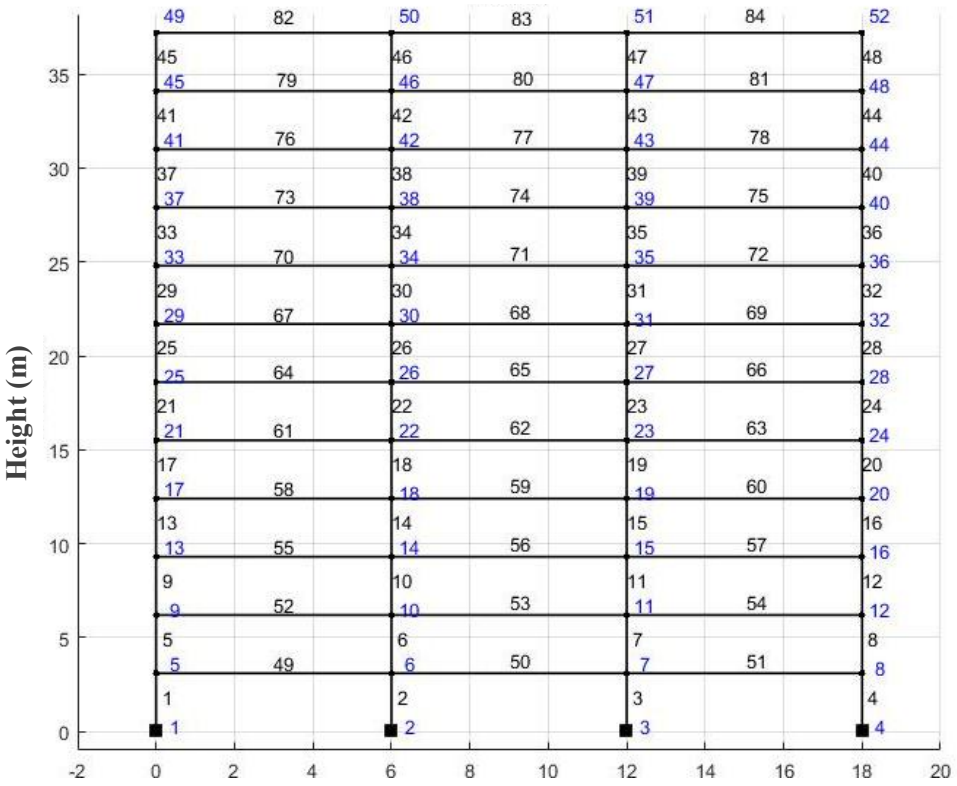

Figure 7. Frame building structure: nodes and elements numbered

frequencies are distributed around a value of approximately 4.0 Hz. Therefore, the first four natural vibration frequencies were chosen as the most representative of the structure's behaviour. Values are shown in Table 4.

Table 4. Comparison of natural frequencies for validation

Modes	Hz	rad/s
1° Mode	0.644	4.047
2° Mode	2.192	13.775
3° Mode	4.445	27.931
4° Mode	7.605	47.782

Figures 9, 10 and 11 and show the first three modes of vibration modes associated with each natural frequency.

The damping coefficients are determined (Eq.12) assuming the critical damping ratio of the first two modes of vibration. Thus, the Rayleigh damping matrix is given by:

$$C = 0.3549[M] + 0.0049[K] \tag{30}$$

Once all the structural parameters necessary to obtain its response to external excitation are determined, two seismic actions generated by the Kanai-Tajimi Spectrum were induced in the model. One of higher intensity, with soil parameters from a region of Santiago, Chile, where there are major events of

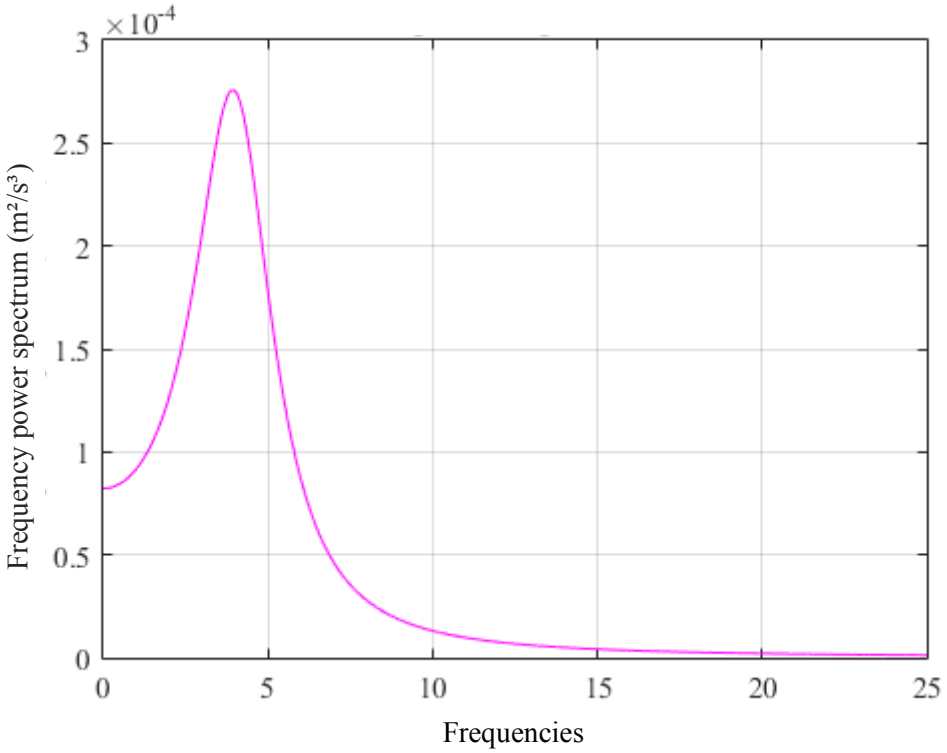

Figure 8. Frequency power spectrum

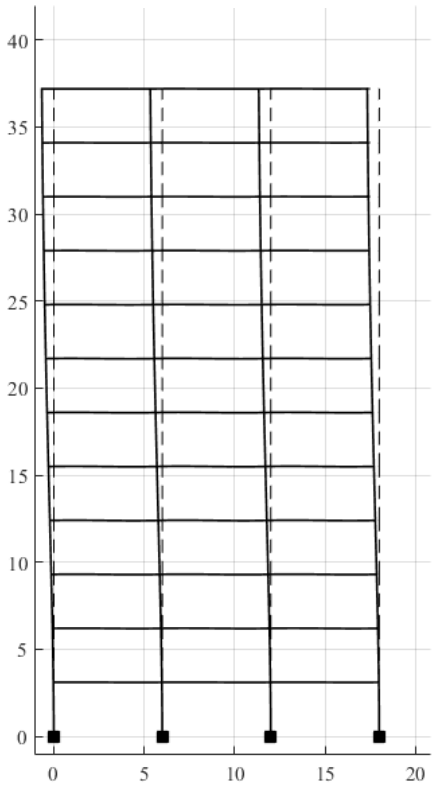

Figure 9. First vibration mode - 0.64 Hz

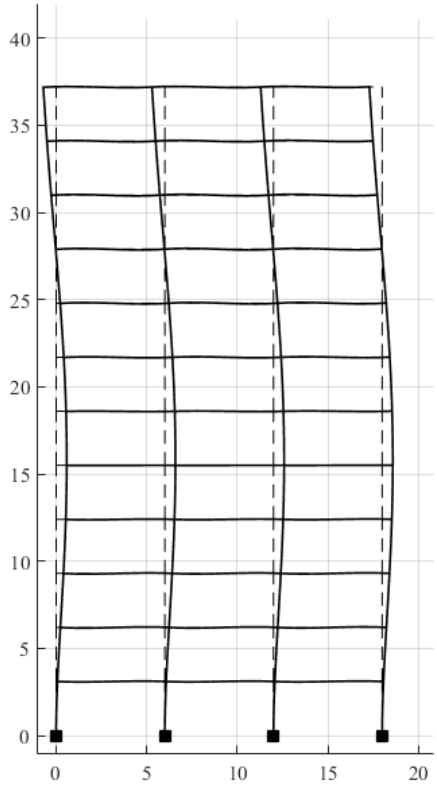

Figure 10. Second vibration mode - 2.19 Hz

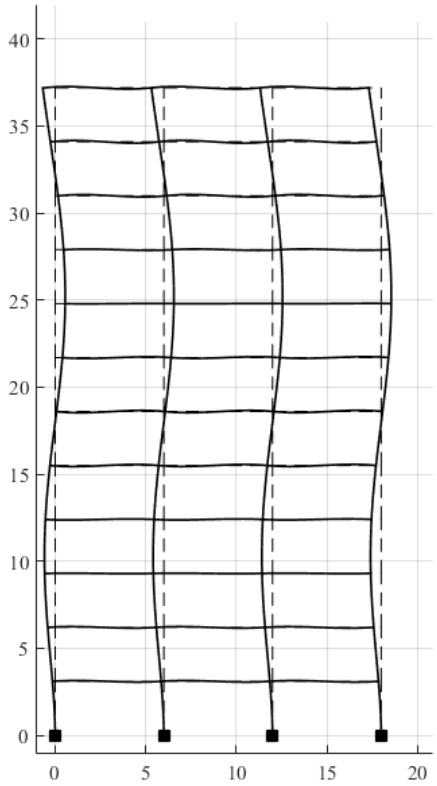

Figure 11. Third vibration mode - 4.45 Hz

seismic nature; and another with lower intensity, located in Acre, Brazil, which was chosen for being the most seismic region in this country [13].

4.1 Dynamic response under seismic action in Chile

The Chilean capital is submitted to high seismicity levels and according to the [14] the PGA of this place is around 0.3g. The accelerogram stations located mainly in the Santiago surroundings point that the site conditions is mostly composed of rocks conforming to [15]. Thus, a ground frequency value of $\omega_g = 27.0 rad/s$ was chosen and for the ground damping, a value of $\xi_g = 0.34$ was considered, according to Kramer [11]. The ground frequency is close to the third natural frequency of the building (Table 4). So, the third mode of vibration is the one being excited.

Figure 12 contemplates the seismic signal, in the time domain, generated by the Kanai-Tajimi spectrum with soil parameters from the region of Santiago.

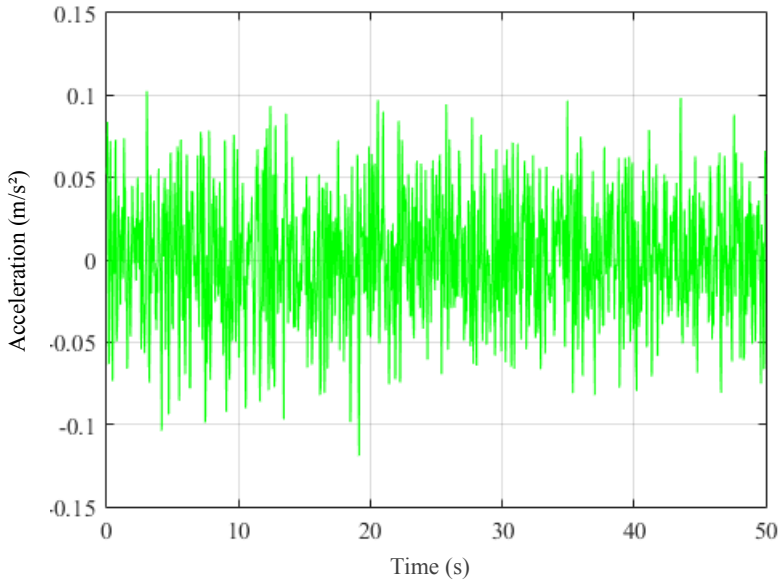

Figure 12. Seismic signal by the Kanai-Tajimi spectrum

Applying the 0.3g PGA, the ground acceleration resulting from the simulated seismic action was determined, as shown in Fig. 13.

With this seismic excitation, the acceleration was applied at the base of the building. To evaluate the structural dynamic response, The graph of the maximum displacement, which happened on the twelfth floor, and the maximum acceleration, were plotted (Fig. 14 and Fig.15, respectively).

For this situation, the maximum displacement is 22.5 cm. The maximum acceleration is 7.8 m/s^2. The relative displacement between the floors of a building is one of the main parameters for evaluating structural stability, according to [13] and [3]. This parameter is presented in Fig.16, in which the columns were named by level.

As in each level there are four bars of the same height, it is considered that the floor has moved in a fully stiff way, taking into account the axial stiffness of the slab. The major relative displacement occurred between the fifth and the fourth floors.

4.2 Dynamic response under seismic action in Brazil

In Acre, in which the soil characteristic is predominantly formed by sedimentary rocks, it was assumed the values of $\omega_g = 22.9 rad/s$ and $\xi_g = 0.30$ conforming to [11] considering an alluvial soil. The PGA for this seismic zone is around 0.15g, according to [13]. Here, also the ground frequency is close to the third natural frequency of the building (see Table 4). So, similar to the Section 4.1, the third

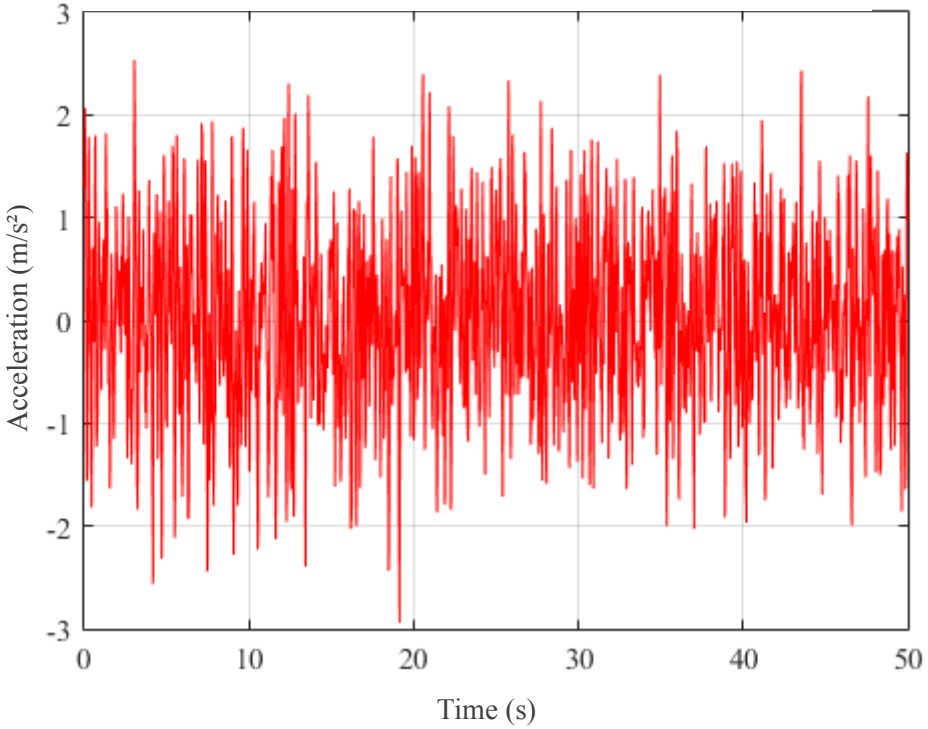

Figure 13. Ground acceleration normalize to PGA

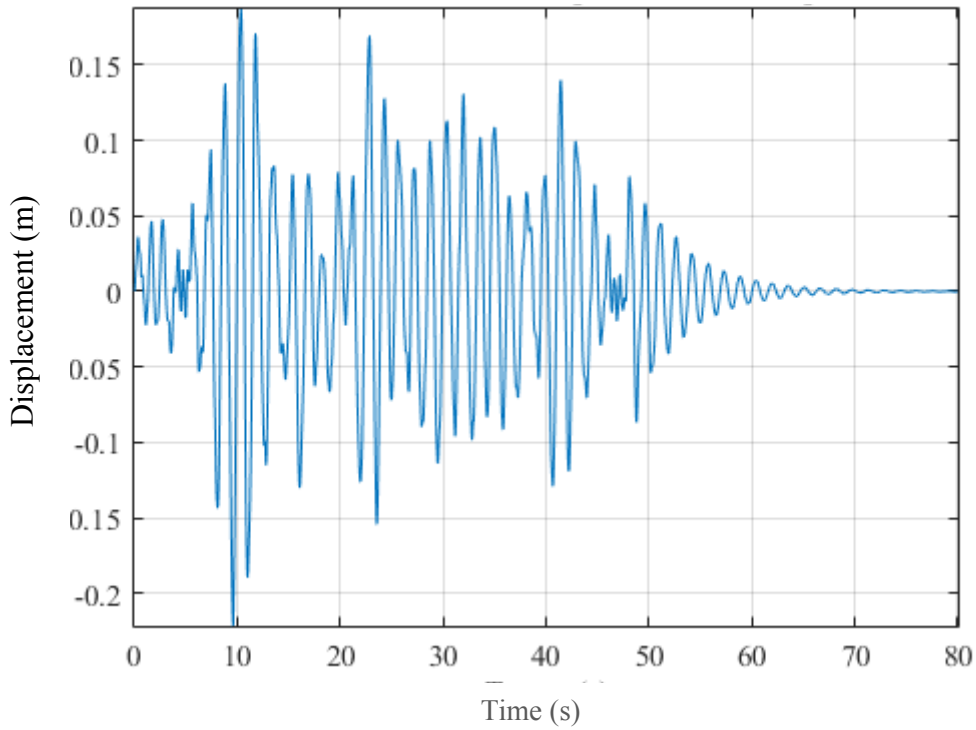

Figure 14. Displacement of the last floor over time

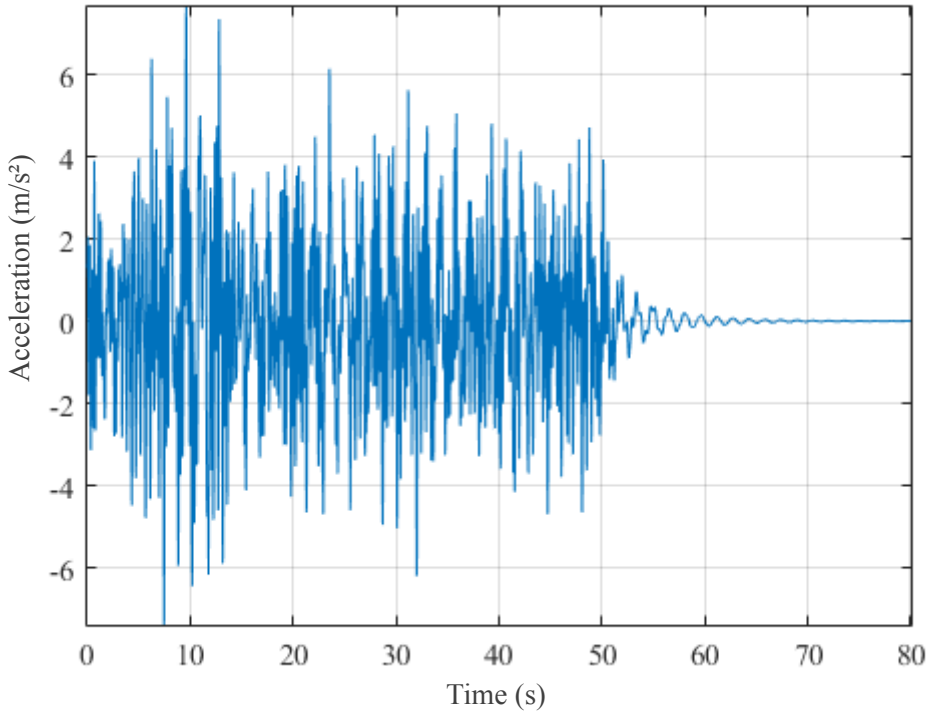

Figure 15. Acceleration of the last floor over time

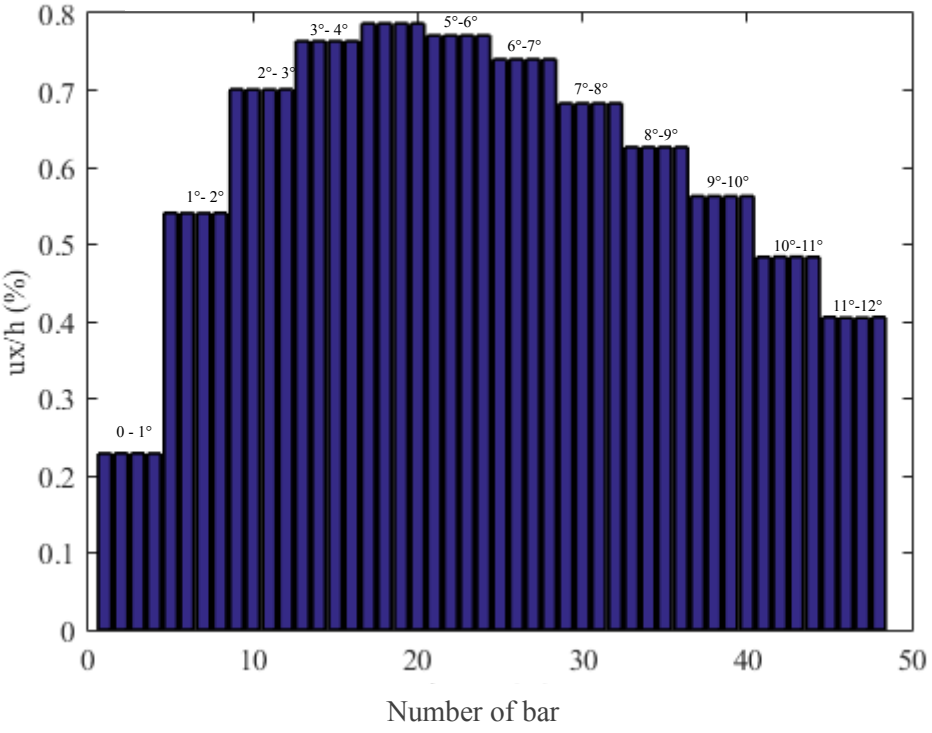

Figure 16. Relative displacement between floors

mode of vibration is the one being excited.

Figure 17 shows the seismic signal obtained from Kanai-Tajimi spectrum using the soil parameters of a region in Acre state, in Brazil. Applying the PGA recommended by [13], the ground acceleration resulting from the simulated earthquake is determined and shown in Fig. 18.

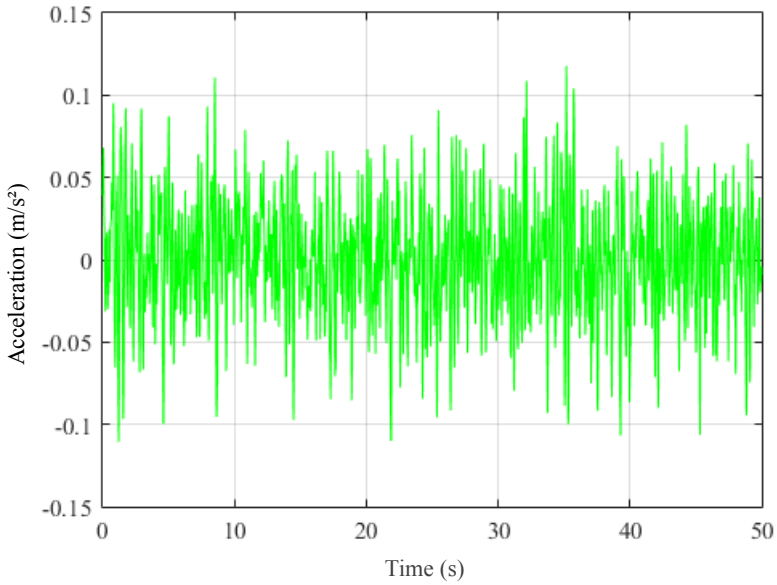

Figure 17. Seismic signal in time domain

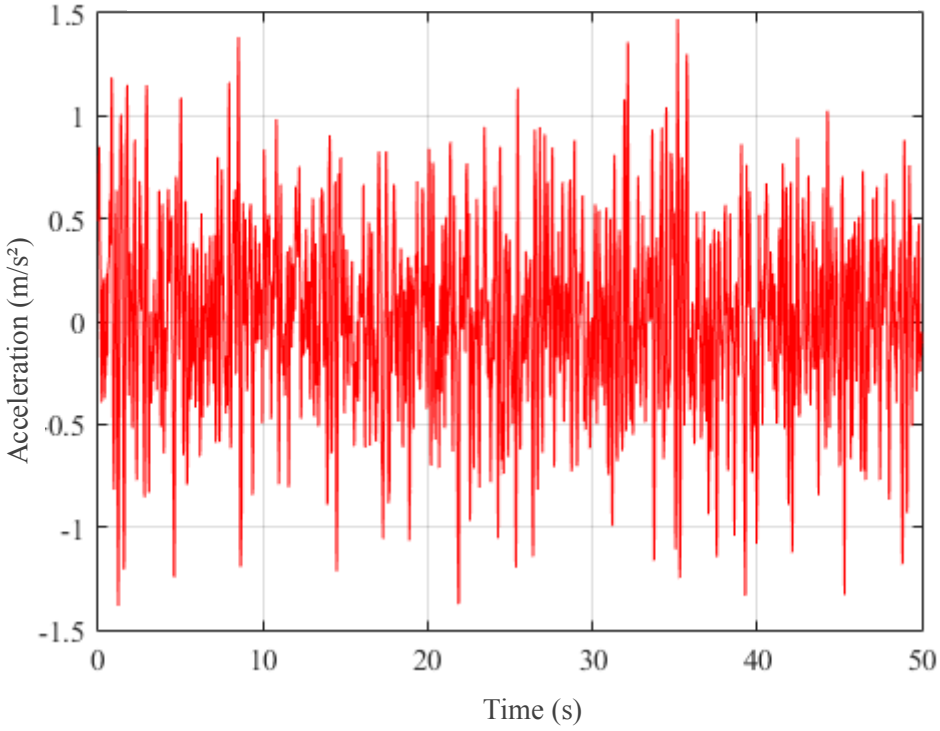

Figure 18. Ground acceleration normalized to PGA

Once the ground acceleration in the time domain normalized to PGA from the local site was generated, the new acceleration was applied to the building base. The dynamic response was obtained. The displacement and acceleration of the 12th floor is shown in Fig.19 and 20, respectively.

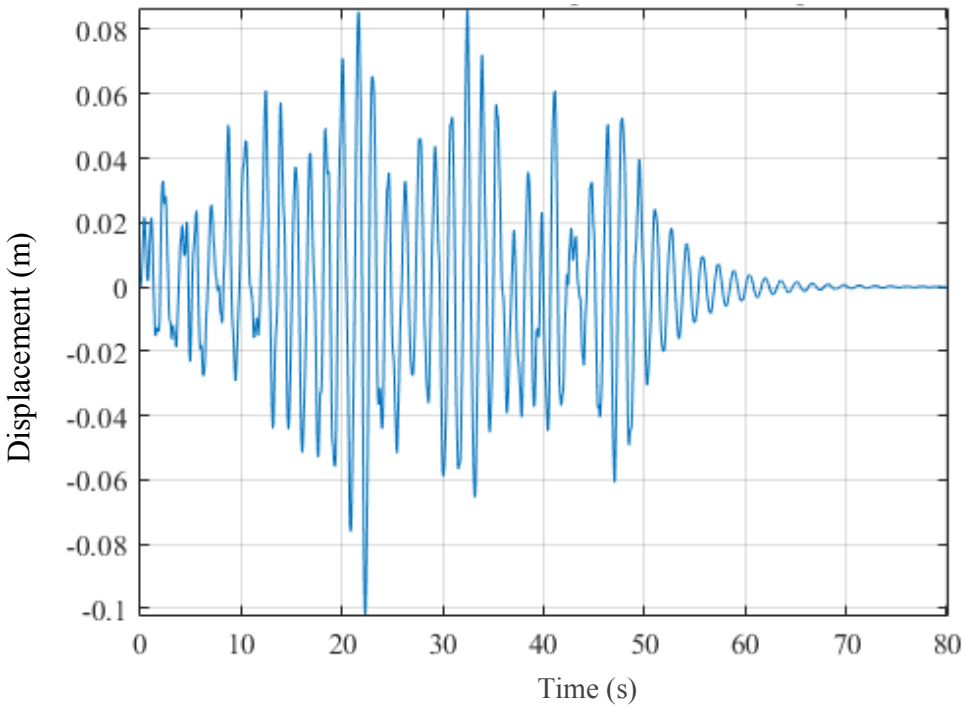

Figure 19. Highest pavement displacement versus time

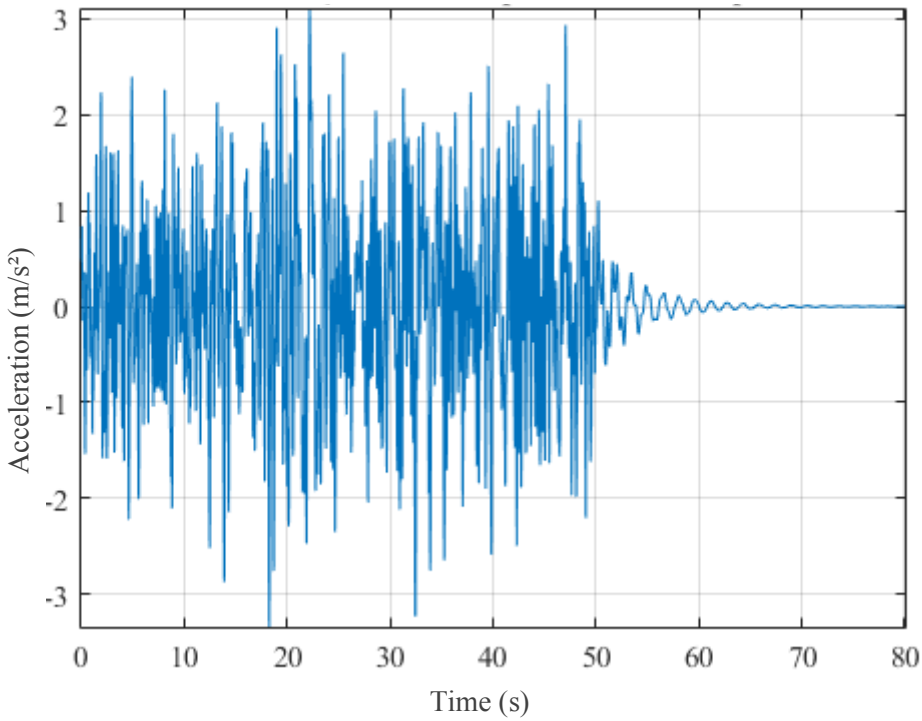

Figure 20. Highest pavement acceleration versus time

The maximum absolute displacement and acceleration of the structure,respectively, are 10.20cm and 3.203 m/s^2.

The relative displacement factor between the pavements was also verified as shown in Fig. 21.

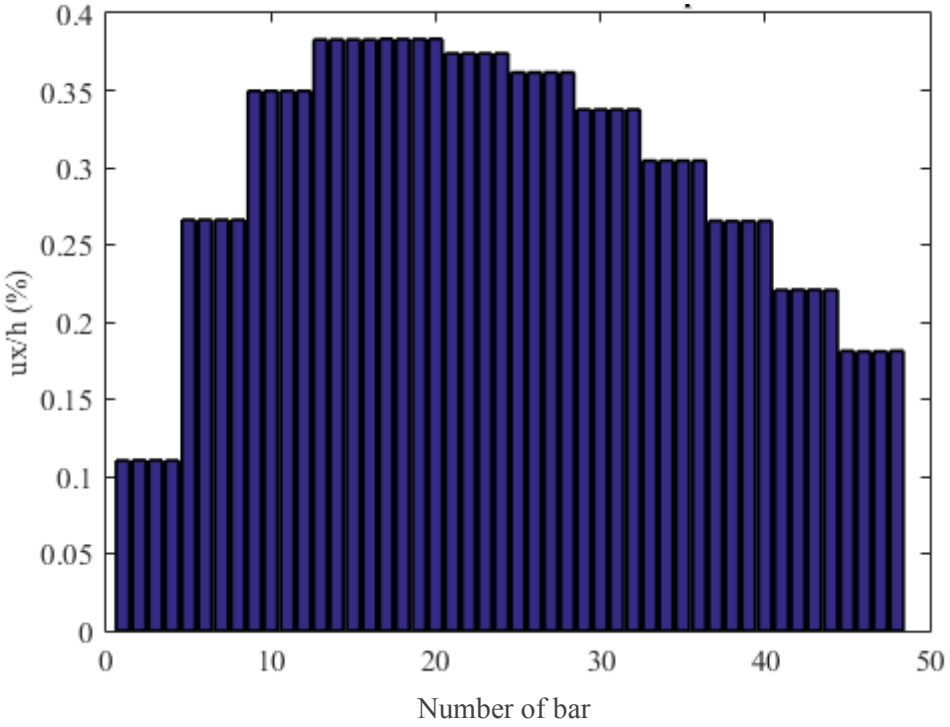

Figure 21. Relative displacement between pavements for the seismic excitation in Brazil

5 Conclusions

After the analysis of both simulated seismic actions, the limits established by both Brazil and Chile's structural codes were compared to the building's response in order to determine if the structure's serviceability would be within each of the limits.

For Santiago seismic case, NCh 433 (INN, 2009) states that the maximum relative displacement should not be greater than the height (in centimeters) between floors multiplied by 0.002, which corresponds to 0.62 cm for this case. This limit was not respected since the maximum displacement was approximately 2.48 cm (0.8 percent of the height between floors as shown in Figure 16).

For Brazilian seismic case, the limit established by NBR 15421 [13], considering the site conditions analyzed and a building category II, is defined as 0.015 of the height (in centimeters) between floors, which corresponds to 4.65 cm. The maximum value from the dynamic response was 1.15 cm (0.37% of the height between floors, 21).

The results indicate that the local soil properties influence on the excitation dynamic properties. The major damages were obtained in the first case studied since the frequency of this site condition were closest to the natural frequencies of the first three vibration modes of the structure. .

Acknowledgements

The authors are grateful to CAPES and CNPq for the scholarship concession and to PROPESQ-UFRGS for providing financial support.

References

[1] Clough, R. & Penzien, J., 1995. *Dynamics of structures*. Inc.

[2] Miguel, L. F. F., Miguel, L. F. F., & Lopez, R. H., 2016. Simultaneous optimization of force and placement of friction dampers under seismic loading. *Engineering Optimization*, vol. 48, n. 4, pp. 582–602.

[3] , 2014. Nbr 6118 - projeto de estruturas de concreto. Rio de Janeiro. Associação Brasileira de Normas Técnicas.

[4] Paz, M., 1985. *Structural dynamics*. Springer.

[5] Soriano, H. L., 2014. *Introdução à dinâmica das estruturas*. Elsevier, Rio de Janeiro.

[6] Troian, S. P., 2018. Sobre a resposta estrutural dinâmica de uma torre estaiada de linha de transmissão submetida a ventos do tipo eps. Master's thesis.

[7] Gomez, A. L. Z., 2007. *Controle de vibrações em edifícios submetidos à ação de cargas dinâmicas utilizando amortecedor de massa sintonizando na forma de pêndulo*. PhD thesis, Universidade de Brasília, Brasília.

[8] Kanai, K., 1961. An empirical formula for the spectrum of strong earthquake motions. *Bulletin Earthquake Research Institute University of Tokyo*, vol. 39, pp. 85–95.

[9] Tajimi, H., 1960. A statistical method of determing the maximum response of a building structure during an earthquake. pp. 781–797.

[10] Shinozuka, M. & Jan, C.-M., 1972. Digital simulation of random processes and its applications. *Journal of sound and vibration*, vol. 25, n. 1, pp. 111–128.

[11] Kramer, S., 1996. *Geotechnical earthquake engineering*, chapter Strong ground motion, pp. 672. Prentice Hall, Inc.

[12] Bathe, K.-J., 1996. *Finite element procedures*. Klaus-Jurgen Bathe.

[13] NBR, A., 2006. 15421: Projeto de estruturas resistentes a sismos-procedimento. *Rio de Janeiro, Brasil:[sn]*.

[14] 433, N., 2009. Nch 433 - diseño sísmico de edifícios.

[15] Liberatore, L., Sorrentino, L., & Liberatore, D., 2012. Engineering analysis of ground motion records of chile, 2010 earthquake. In *Proc. of the 15th World Conf. on Earthq. Eng*.